Wrinkled Flames and Cellular Patterns

Jeong-Mo Hong[*]
Stanford University

Tamar Shinar[*]
Stanford University

Ronald Fedkiw[†]
Stanford University
Industrial Light+Magic
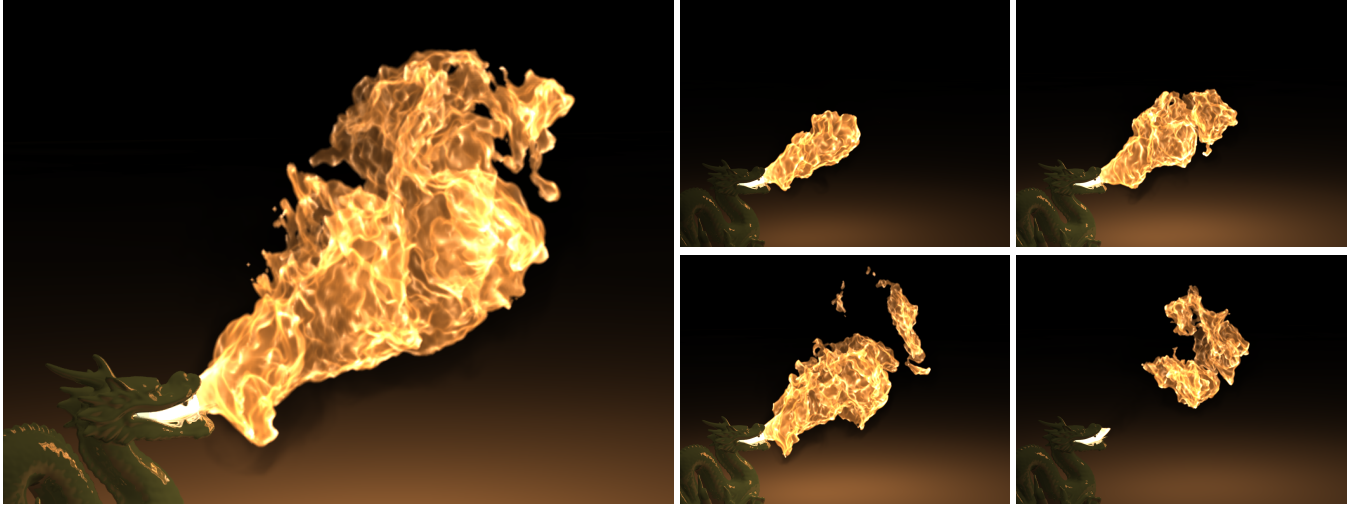
Figure 1: A dragon emits a flame, computed with the third order DSD equations coupled to the Navier-Stokes equations.

Abstract

We model flames and fire using the Navier-Stokes equations combined with the level set method and jump conditions to model the reaction front. Previous works modeled the flame using a combination of propagation in the normal direction and a curvature term which leads to a level set equation that is parabolic in nature and thus overly dissipative and smooth. Asymptotic theory shows that one can obtain more interesting velocities and fully hyperbolic (as opposed to parabolic) equations for the level set evolution. In particular, researchers in the field of detonation shock dynamics (DSD) have derived a set of equations which exhibit characteristic cellular patterns. We show how to make use of the DSD framework in the context of computer graphics simulations of flames and fire to obtain interesting features such as flame wrinkling and cellular patterns.

CR Categories: I.3.5 [Computer Graphics]: Computational Geometry and Object Modeling—Physically based modeling

Keywords: fire, flame, combustion, cellular patterns

[*]e-mail: {jeongmo,shinar}@stanford.edu
[†]e-mail: fedkiw@cs.stanford.edu

1 Introduction

While various researchers have considered physics-based simulation of smoke and water, significantly fewer have considered fire and explosions. Likewise, special effects companies have not disseminated much information on physically based methods for fire and explosions (e.g. [Lamorlette and Foster 2002], [Geiger et al. 2005] and [bin Zafar et al. 2004] based on [Nguyen et al. 2002]). Since the physically based simulation of fire and explosions is useful for obvious financial and safety reasons, more research is required in this area.

Researchers in the combustion community have struggled with the modeling of flames and fire especially because of the complex nature of the chemical reactions governing these phenomena. One approach, initiated some time ago (see e.g. [Markstein 1964]), was to develop asymptotic theory to model chemical reactions as if they occurred across an infinitely thin surface resulting in a partial differential equation called the G-equation. Later, numerical methods were proposed by [Osher and Sethian 1988] (although there was earlier work by [Dervieux and Thomasset 1979; Dervieux and Thomasset 1981]) for the simulation of surfaces which move with a combination of normal velocity and curvature terms, basically identical to the G-equation. [Nguyen et al. 2001] coupled the numerical methods of [Osher and Sethian 1988] for the level set equation to the Navier-Stokes equations in order to model two-phase incompressible flames. This model was shown to be applicable to computer graphics simulations of fire and flames in [Nguyen et al. 2002].

Significant research has occurred in the combustion community since [Markstein 1964] especially since modeling these thin reaction fronts both theoretically and numerically is expensive requiring methods for multiscale phenomena, significant computational resources, etc. In fact, detonation as a form of combustion is one of the driving problems for the acquisition and utilization of large supercomputers by facilities such as Los Alamos and Livermore na-
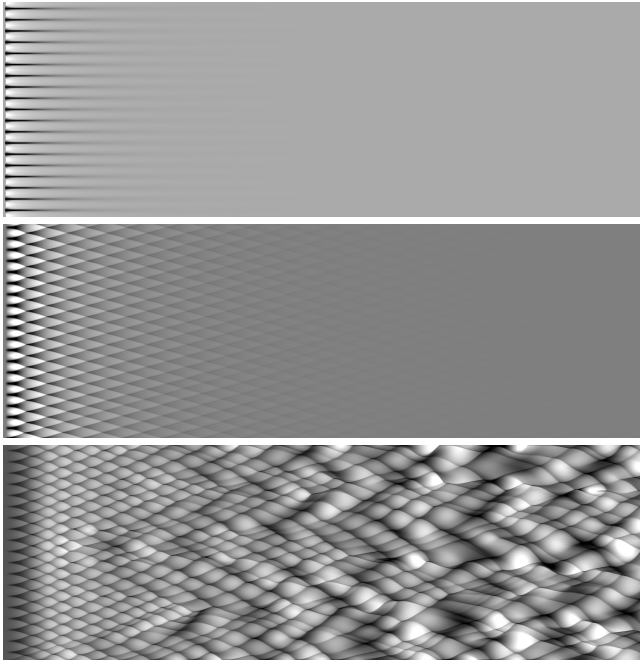
Figure 2: Simulated smoked foils. Lighter regions correspond to a slower flame speed, and the flame moves from left to right in each figure. An initial sine wave perturbation is smoothed out by the first order DSD equations (top) and the second order DSD equations (middle), whereas interesting cellular patterns develop for the third order DSD equations (bottom).

tional laboratories. A particularly interesting area of asymptotic research is detonation shock dynamics [Yao and Stewart 1996; Aslam et al. 1996] where researchers derived equations that admit cellular patterns. DSD theory shows that the normal plus curvature driven interface velocities used in [Nguyen et al. 2001; Nguyen et al. 2002] result in smooth, diffuse flames which is obvious considering the fact that curvature driven motion leads to a parabolic partial differential equation. The normal plus curvature driven interface velocity is consistent with first order DSD theory, but DSD theory also contains second and third order equations which are hyperbolic (not parabolic) and thus not inherently diffusive. Note that hyperbolic differential equations are computationally more efficient to simulate than their parabolic counterparts, because they possess a significantly less restrictive CFL condition. More importantly, third order DSD theory yields a set of partial differential equations that produce complex time-coherent cellular patterns.

Although low speed fire and flames (i.e. deflagrations) differ in many ways from their higher speed shock wave coupled counterparts (i.e. detonations), the highly intricate time-coherent cellular patterns produced by DSD are visually compelling and thus the focus of our work. From the standpoint of computer graphics applications, obtaining a more interesting velocity for the level set surface allows for more visually interesting fire and flames, while low speed phenomena are still faithfully modeled with the incompressible Navier-Stokes equations. Therefore, we extend the work of [Nguyen et al. 2002] from the parabolic inherently smooth flame velocities to the more interesting hyperbolic third order DSD approximations that yield cellular patterns and flame wrinkling.

2 Previous Work

Previous flame models in computer graphics include [Inakage 1989; Perry and Picard 1994; Chiba et al. 1994; Stam and Fiume 1995;
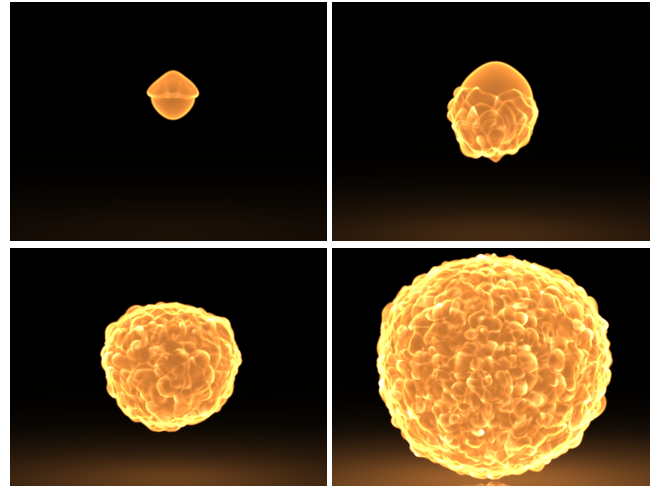
Figure 3: Four images from the time evolution of a level set surface using the third order DSD equations. Note that the Navier-Stokes equations are not used in this example, rather it illustrates that the cellular patterns are produced by the DSD augmented level set equations without the need for vorticity confinement or other turbulence models.

Bukowski and Sequin 1997; Beaudoin et al. 2001; Melek and Keyser 2002; Adabala and Hughes 2004]. In addition, simulation of explosions was addressed in [Musgrave 1997; Mazarak et al. 1999; Neff and Fiume 1999; O'Brien and Hodgins 1999; Yngve et al. 2000; Feldman et al. 2003; Geiger et al. 2003; Rasmussen et al. 2003; Geiger et al. 2005]. Many authors have focused on the rendering of fire and flames and we refer the interested reader to [Rushmeier et al. 1995; Pegoraro and Parker 2006] for example. In [Melek and Keyser 2003; Melek and Keyser 2005; Losasso et al. 2006a], fire was considered in the context of eroding solid objects, and [Melek and Keyser 2006] also modeled the crumpling of solids based on heat. Similarly, [Losasso et al. 2006b] simulated burning liquids, and [Zhao et al. 2003] described a model for the propagation of fire along solid surfaces.

3 Flame Speed

We first consider the flame front velocities used in [Nguyen et al. 2002] which have the form

$$D = a - b\kappa \qquad (1)$$

where a and b are positive constants and κ is the local mean curvature of the flame surface. Using the level set function ϕ, we can define the local unit normal $\mathbf{n} = \nabla\phi/|\nabla\phi|$ and the curvature $\kappa = -\nabla \cdot \mathbf{n}$. The standard equation for level set evolution is

$$\phi_t + \mathbf{w} \cdot \nabla\phi = 0, \qquad (2)$$

where $\mathbf{w} = ((u_n)_f - D)\mathbf{n}$. The $(u_n)_f$ term denotes the normal velocity of the unreacted fuel which we ignore for the rest of Section 3, leaving the discussion of coupling to the Navier-Stokes equations to Section 4. When ϕ is a signed distance function, $\mathbf{n} = \nabla\phi$, $\kappa = -\triangle\phi$, and setting $a = 0$ yields the parabolic heat (diffusion) equation $\phi_t = b\triangle\phi$, which smooths out detail on the flame surface. Equation (2) can be made hyperbolic by setting $b = 0$, but still does not produce interesting cellular patterns.

Classical detonation theory describes the velocity of a one-dimensional steady detonation wave called the Chapman-Jouguet
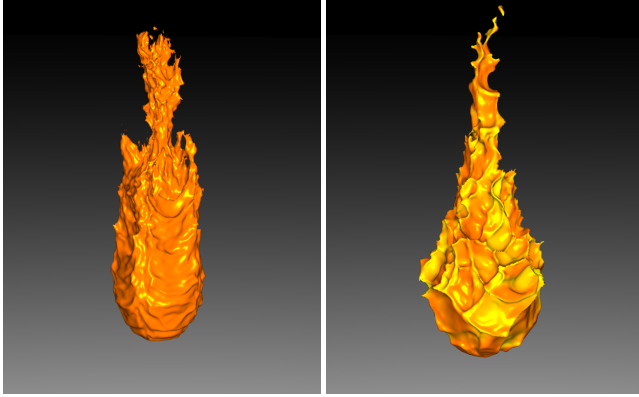
Figure 4: A technical illustration of flame cores computed using the full coupling of the DSD equations to the Navier-Stokes equations. The first order parabolic DSD equations are shown on the left, while the third order DSD equations are shown on the right. We used different colors to represent different flame speeds emphasizing the fact that the first order equations do not produce and accentuate cellular patterns. Note that in the first order result, we have set $b = 0$ removing the parabolic curvature term and used vorticity confinement in order to get as much detail as possible, but even so distinct cellular patterns are not generated.

(CJ) detonation. DSD augments this theory by considering deviations in curvature from a planar Chapman-Jouguet detonation front as well as unsteady detonations velocities, thus providing a fully multidimensional detonation model. The important parameters are the detonation speed D, its material derivatives (e.g. $\dot{D}$ and $\ddot{D}$) and the geometry of the shock surface (e.g. κ and $\dot{\kappa}$). The first order relation, termed the $D - \kappa$ relation, is given in equation (1). The second order relation, $\dot{D} - D - \kappa$, considers the first time derivative of the detonation velocity via

$$D_t + \mathbf{w} \cdot \nabla D = \dot{D} \qquad (3)$$
$$\dot{D} = -\alpha\kappa + \beta(D - D_{CJ}) \qquad (4)$$

where D_{CJ} is the planar detonation velocity predicted by the one-dimensional Chapman-Jouguet detonation theory.

While the second order DSD equations are hyperbolic, it is the third order theory utilizing a $\ddot{D} - \dot{D} - D - \dot{\kappa} - \kappa$ relation which results in a hyperbolic partial differential equation that generates self-sustaining cellular patterns. The equations for third order DSD theory are (see e.g. [Aslam 1996]),

$$D_t + \mathbf{w} \cdot \nabla D = \dot{D} \qquad (5)$$
$$\dot{D}_t + \mathbf{w} \cdot \nabla \dot{D} = \ddot{D}(\dot{D}, D, \dot{\kappa}, \kappa) \qquad (6)$$

where $\dot{\kappa}$ is the material derivative of the curvature $\dot{\kappa} = \kappa_t + \mathbf{w} \cdot \nabla \kappa$. These equations state that D and $\dot{D}$ are advected with the interface velocity and integrated with the source terms on the right hand side. Equation (5) is similar to equation (3) except that instead of obtaining $\dot{D}$ from equation (4), equation (5) obtains it from equation (6). The system of equations (2), (5) and (6) is closed by defining

$$\ddot{D} = -c_1\alpha^2(D - D_{CJ}) - c_2\alpha\dot{D} - c_3\alpha^2 L_{CJ} - c_4\dot{\kappa} \qquad (7)$$
$$\alpha = e^{\mu\theta(D - D_{CJ})}, \qquad L_{CJ} = \ln|1 + c_5\theta\kappa/\alpha|$$

where θ is the activation energy. The first two terms of equation (7) are elastic and damping terms describing the oscillatory motion of D about D_{CJ}. The third term is a curvature forcing term which accentuates the variations in curvature of the front. In particular,
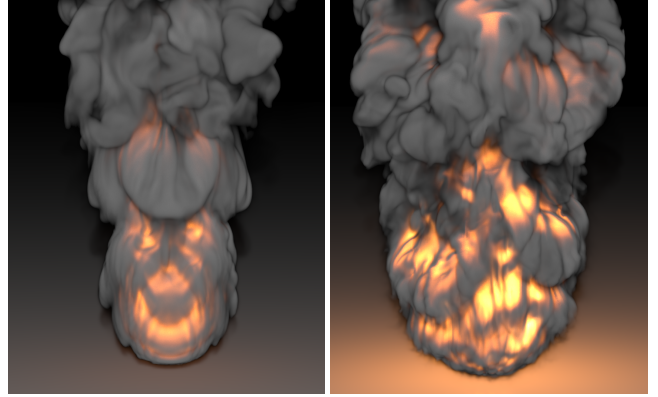
Figure 5: These simulations correspond to those shown in Figure 4, except that we render the smoke density field instead of illustrating the flame core. Again, note the improved result using third order DSD theory.

since $\kappa > 0$ corresponds to regions where $D < D_{CJ}$, that term further decelerates D, whereas regions with $\kappa < 0$ where $D > D_{CJ}$ are accelerated. The last term involving $\dot{\kappa}$ is a damping term.

Although the coefficients c_1 to c_5 and μ are functions of two material-dependent parameters (namely the polytropic exponent of the material and the Mach number of the Chapman-Jouguet detonation), in practice one can tune them independently to carve the desired cellular patterns in the flame. Furthermore, θ can be considered as a part of $\mu\theta$ and $c_5\theta$ instead of an independent degree of freedom. After setting D_{CJ} to the desired base flame speed and setting c_1 and c_2 for the desired elasticity and damping about D_{CJ}, we found that tweaking the curvature forcing term, c_3, gives us sufficient control of the cellular patterns in terms of simulation detail. The curvature damping term including c_4 was essential for the delicate control of cellular patterns for non-coupled simulations, but we found it can be omitted for coupled simulations because the curvature forcing term dominates. $\mu\theta$ was used to limit the deviation of D from D_{CJ} and $c_5\theta$ determined the sensitivity of L_{CJ} to curvature. It was useful to normalize $c_5\theta$ by Δx when testing coefficients with various grid resolutions. We present the simulation coefficients we used in Table 3.

Each time step, we first advect ϕ, D, $\dot{D}$ and κ forward in time using the velocity field $\mathbf{w}$ ignoring source terms. Although special techniques are typically used to evolve the level set equation, the DSD related parameters D, $\dot{D}$ and κ can be treated more simply with semi-Lagrangian advection or a higher order accurate variant [Stam 1999; Kim et al. 2006; Selle et al. 2007]. As is typical the fast marching method can be used to maintain the signed distance property of ϕ, whereas the DSD related scalars need to be extended constant normal to the interface. This extrapolation in the normal direction is similar to the one-way extrapolation done for the velocity field in [Enright et al. 2002]. To evaluate the source terms, we first compute the new curvature field $\kappa^{n+1} = \kappa(\phi^{n+1})$ using the new value of the level set function. Then we compute $\dot{\kappa} = (\kappa^{n+1} - \kappa^\star)/\Delta t$ where $\kappa^\star$ is the value obtained by advecting the time n curvature field forward in time. Next the source term $\ddot{D}$ is evaluated using $\dot{\kappa}$ and the advected values of D, $\dot{D}$, and κ (i.e. $D^\star$, $\dot{D}^\star$ and $\kappa^\star$). That is, $\ddot{D} = \ddot{D}(D^\star, \dot{D}^\star, \kappa^\star, \dot{\kappa})$. The advected value of $\dot{D}$ is then augmented by $\Delta t \ddot{D}$, and subsequently the advected value of D is augmented by $\Delta t \dot{D}$. See Table 1 for pseudocode.

A widely used experimental technique for studying the cellular structure exhibited by gaseous detonations is the smoked foil technique, in which a controlled detonation is carried out in a tube lined with soot coated metal foil. As the detonation propagates through
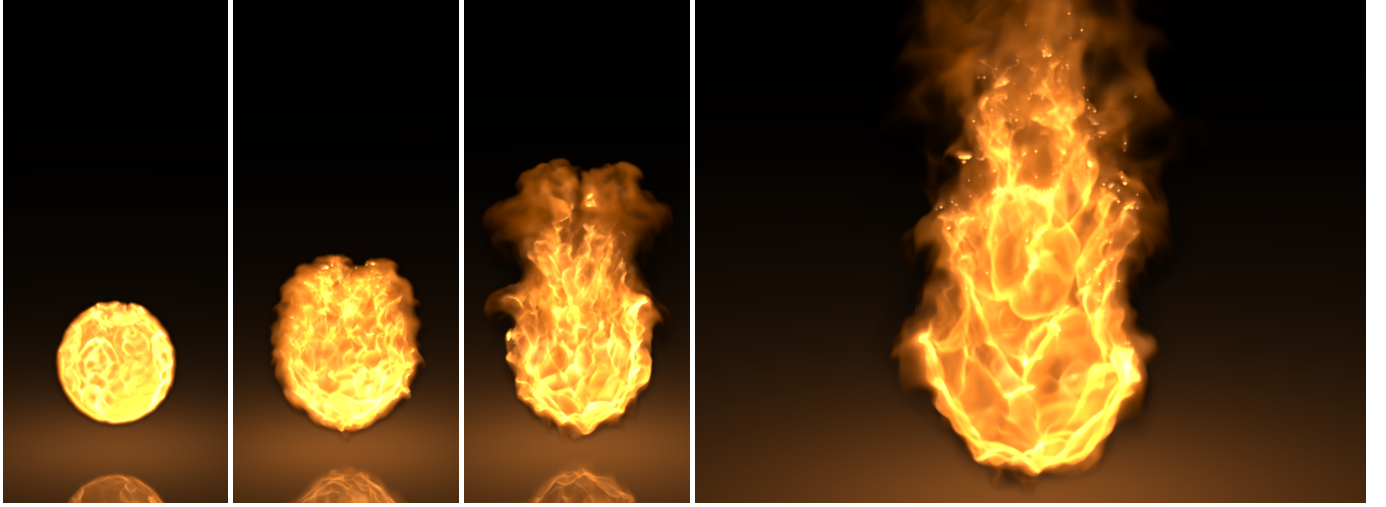
Figure 6: Fireball generated by coupling the third order DSD equations to the Navier-Stokes equations.

the tube, the pressures generated leave an imprint on the foil. A similar process can be simulated numerically using the DSD equations. Figure 2 is generated by recording the reaction speed as the detonation front crosses over each grid point, moving from left to right in the figures. Note the striking difference between the first, second and third order DSD equations. While the initial perturbations are smoothed out by the first and second order equations, they persist and are amplified for the third order equations. Figure 3 shows the time evolution of a three-dimensional level set surface using the third order DSD equations. Note that the complex cellular patterns in Figure 2, bottom, and Figure 3 were obtained using only equations (2), (5), (6) and (7) without any consideration of the Navier-Stokes equations. The ability of DSD theory to produce such interesting phenomena without the aid of the Navier-Stokes equation is due to the fact that the equations themselves were asymptotically derived from the Navier-Stokes equations.

4   Coupling with Navier-Stokes Equations

Now that we have demonstrated the ability of DSD theory to produce level set surfaces with interesting cellular patterns, in this section we couple the level set/DSD evolution to the three-dimensional Navier-Stokes equations as in [Nguyen et al. 2002]. The equations for inviscid incompressible flow are given by

$$\mathbf{u}_t + (\mathbf{u} \cdot \nabla)\mathbf{u} + \nabla p/\rho = \mathbf{f} \qquad (8)$$

along with the divergence-free condition $\nabla \cdot \mathbf{u} = 0$, where $\mathbf{u}$ is the velocity, p is the pressure, ρ is the density, and $\mathbf{f}$ denotes body forces such as gravity, buoyancy and vorticity confinement. The conversion of mass due to the reaction induces discontinuities in pressure and normal velocity across the interface that must satisfy interface jump conditions (derived through balancing the mass and momentum flux across the interface) given by

$$[\rho(u_n - w_n)] = 0 \qquad (9)$$
$$[\rho(u_n - w_n)^2 + p] = 0, \qquad (10)$$

where $u_n = \mathbf{u} \cdot \mathbf{n}$, $w_n = \mathbf{w} \cdot \mathbf{n}$, and "$[\cdot]$" denotes the jump across the interface [Nguyen et al. 2001]. Since ρ is discontinuous across the interface, these equations imply that u_n and p are discontinuous as well. To obtain accurate derivatives across interfaces with sub-grid accuracy, discontinuous variables are extrapolated using continuous variables based on their physical properties. See [Nguyen et al. 2002; Hong and Kim 2005; Losasso et al. 2006b] for implementation details.

To obtain a better temperature profile for both buoyancy and rendering, we additionally consider the jump condition implied by conservation of energy

$$[e + (u_n - w_n)^2/2 + p/\rho] = 0 \qquad (11)$$

where e is the internal energy per unit mass. For a calorically perfect gas, $de = c_v dT$ where c_v is the specific heat at constant volume and T is the temperature. Integrating this relationship, setting the arbitrary zero point energy to zero at 0K, one obtains $e = c_v T$ which can be used to rewrite the jump condition as

$$[c_v T + (u_n - w_n)^2/2 + p/\rho] = 0 \qquad (12)$$

noting that c_v is different for the reacted and unreacted materials.

As a summary of the whole DSD algorithm, we present the pseudocode in Table 1 illustrating that the implementation is a simple extension to [Nguyen et al. 2002]. The Navier-Stokes equations (8) are solved exactly as in [Nguyen et al. 2002] except that $\mathbf{w}$ is defined slightly differently in the sense that D is no longer defined by equation (1) but instead is defined by equations (5), (6) and (7). Equation (5) is solved for D in the same way as equation (2) is solved for ϕ except that there is a source term so it requires a separate step of addition. That source term obeys equation (6) which is the same advection as equation (2) for the level set as is the equation for κ. Once again equation (6) has a source term which is evaluated and added to $\dot{D}$. Note that the values of $\dot{D}, D, \dot{\kappa}, \kappa$ are plugged into the source term in equation (6) via equation (7) which is evaluated by simple arithmetic operations.

Figures 4, 5 and 6 illustrate the results obtained when coupling the DSD equations to the full Navier-Stokes equations. In particular, figures 4 and 5 contrast the differences between the first order DSD equations and the third order DSD equations.

5   Examples

The examples presented were computed using the third order DSD equations coupled to the Navier-Stokes equations. We used vorticity confinement as in [Fedkiw et al. 2001] (vortex particles [Selle et al. 2005] could also be used) in the fuel and product regions. In order to extend the expanse of the fuel we advect particles that act to increase the divergence in the fuel region as in [Feldman et al. 2003]. We use photon mapping for the fire lighting and a blackbody radiation model for the fuel and gaseous products.
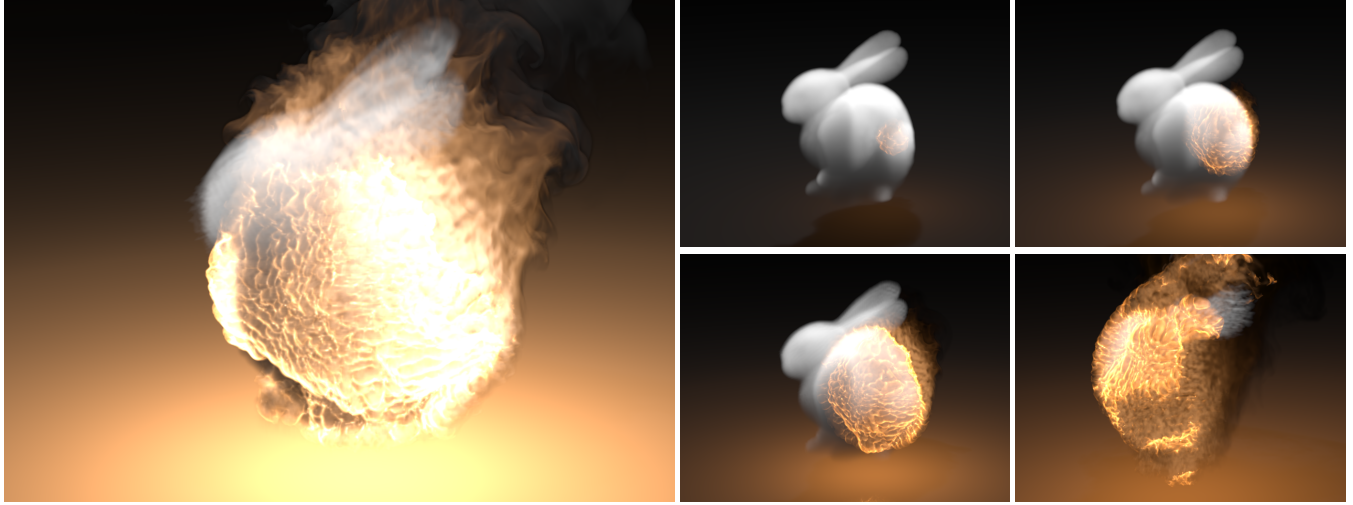
Figure 7: Fire propagates through a gaseous fuel in the shape of a bunny.

```
Main_Loop( )
{
    Update_D_With_DSD(. . . );
    Previous_Fire_Simulator(. . . ,D); //[Nguyen et al. 2002]
}

Update_D_With_DSD(. . . )
{
    //[Stam 1999; Kim et al. 2006; Selle et al. 2007]
    Advect ϕⁿ,Dⁿ,Ḋⁿ,κⁿ to get ϕⁿ⁺¹,Dⁿ⁺¹,Ḋⁿ⁺¹,κ*;

    for(Interfacial_Nodes)
    {
        κ̇ = (κⁿ⁺¹ − κ*)/Δt;
        δ = Dⁿ⁺¹ − D_CJ;
        α = exp(μθ ∗ δ);
        L_CJ = ln|1 + c₅θ ∗ κⁿ⁺¹/α|;

        //Compute RHS of equation (6)
        D̈ = −c₁ ∗ α² ∗ δ − c₂ ∗ α ∗ Ḋⁿ⁺¹ − c₃ ∗ α² ∗ L_CJ − c₄ ∗ κ̇;

        //Euler step of D and Ḋ
        Ḋⁿ⁺¹+=D̈ ∗ Δt;
        Dⁿ⁺¹+=Ḋⁿ⁺¹ ∗ Δt;
    }
    Extrapolate Dⁿ⁺¹,Ḋⁿ⁺¹,κⁿ⁺¹;
}
```

Table 1: Pseudocode for the DSD algorithm as an extension to the previous fire simulator of [Nguyen et al. 2002].

Figure 1 depicts fire emanating from a dragon. We rendered the smoke in a dark fashion to accentuate the time-coherent cellular patterns. In Figure 7, we begin with an initial gaseous fuel density in the shape of a bunny. Then, the fuel is ignited at a point and the flame propagates consuming the fuel. Note that this was accomplished with a level set by seeding a product level set near the bunny's tail and only setting a non-zero flame velocity near regions of high fuel density. That is, while one side of the level set still corresponds to products, the other side corresponds to both fuel and non-fuel air with a non-zero flame velocity only near the fuel.

All examples were run on a number of 4 processor 2.6 GHz Opteron

machines and timing results are presented in Table 2. The DSD times include level set advection and reinitialization and account for only a few percent of the computational cost. Note that the source terms on the right hand side of equations (5) and (6) integrated with the explicit Euler method posed no stability issues with reasonable CFL numbers.

6   Conclusion

In this paper we focused on a method for generating improved velocities for a level set representation of the flame front. Using DSD theory we were able to promote and sustain cellular patterns in our flames obtaining new visual phenomena for computer graphics generated fire.

Acknowledgements

References

ADABALA, N., AND HUGHES, C. E. 2004. A parametric model for real-time flickering fire. In *Proc. of Comput. Anim. and Social Agents (CASA)*.

ASLAM, T., BDZIL, J., AND STEWART, D. S. 1996. Level set methods applied to modeling detonation shock dynamics. *J. Comput. Phys. 126*, 390–409.

ASLAM, T. D. 1996. *Investigations on detonation shock dynamics*. PhD thesis, University of Illinois at Urbana-Champaign.

BEAUDOIN, P., PAQUET, S., AND POULIN, P. 2001. Realistic and Controllable Fire Simulation. In *Proc. of Graph. Interface 2001*, 159–166.

BIN ZAFAR, N., FALT, H., ALI, M. Z., AND FONG, C. 2004. Dd::fluid::solver::solverfire. In *SIGGRAPH 2004 Sketches & Applications*, ACM Press.

BUKOWSKI, R., AND SEQUIN, C. 1997. Interactive Simulation of Fire in Virtual Building Environments. In *Proc. of SIGGRAPH 1997*, ACM

	Number of frames	Total time	Mean time per frame	DSD time per frame	CFL number	Grid resolution
Figure 1	521	68 hr	469 sec	5 %	2	$300 \times 250 \times 250$
Figure 6	300	24 hr	291 sec	6 %	2	$200 \times 300 \times 200$
Figure 7	225	50 hr	800 sec	6 %	1.5	$250 \times 250 \times 250$

Table 2: Simulation times

	D_{CJ}	a	b	α	β	c_1	c_2	c_3	c_4	$\mu\theta$	$c_5\theta\Delta x$	Δx	Grid size
Figure 2 (top)		1	0.01									0.08	120×40
Figure 2 (middle)	1			1	0.1							0.08	120×40
Figure 2 (bottom)	1					0.2	0.1	87.5	0.625	1	0.01	0.08	120×40
Figure 1	0.2					1	0.1	100	0	2	2.5	0.04	$12 \times 10 \times 10$
Figure 3	0.1					0.01	0.001	0.013	0.002	1	1	0.0267	$8 \times 8 \times 8$
Figure 6	0.2					10	0.1	100	0	2	2.5	0.01	$2 \times 3 \times 2$
Figure 7	0.2					3	0.3	300	0	2	2.5	0.024	$6 \times 6 \times 6$

Table 3: Simulation parameters

Press / ACM SIGGRAPH, Comput. Graph. Proc., Annual Conf. Series, ACM, 35–44.

CHIBA, N., MURAOKA, K., TAKAHASHI, H., AND MIURA, M. 1994. Two dimensional Visual Simulation of Flames, Smoke and the Spread of Fire. *J. Vis. and Comput. Anim. 5*, 37–53.

DERVIEUX, A., AND THOMASSET, F. 1979. A finite element method for the simulation of a Rayleigh-Taylor instability. *Lecture Notes in Math. 771*, 145–158.

DERVIEUX, A., AND THOMASSET, F. 1981. Multifluid incompressible flows by a finite element method. *Lecture Notes in Phys. 141*, 158–163.

ENRIGHT, D., MARSCHNER, S., AND FEDKIW, R. 2002. Animation and rendering of complex water surfaces. *ACM Trans. Graph. (SIGGRAPH Proc.) 21*, 3, 736–744.

FEDKIW, R., STAM, J., AND JENSEN, H. 2001. Visual simulation of smoke. In *Proc. of ACM SIGGRAPH 2001*, 15–22.

FELDMAN, B. E., O'BRIEN, J. F., AND ARIKAN, O. 2003. Animating suspended particle explosions. *ACM Trans. Graph. (SIGGRAPH Proc.) 22*, 3, 708–715.

GEIGER, W., RASMUSSEN, N., HOON, S., AND FEDKIW, R. 2003. Big bangs. In *SIGGRAPH 2003 Sketches & Applications*, ACM Press.

GEIGER, W., RASMUSSEN, N., HOON, S., AND FEDKIW, R. 2005. Space battle pyromania. In *SIGGRAPH 2005 Sketches & Applications*, ACM Press.

HONG, J.-M., AND KIM, C.-H. 2005. Discontinuous fluids. *ACM Trans. Graph. (SIGGRAPH Proc.) 24*, 3, 915–920.

INAKAGE, M. 1989. A Simple Model of Flames. In *Proc. of Comput. Graph. Int. 89*, Springer-Verlag, 71–81.

KIM, B.-M., LIU, Y., LLAMAS, I., AND ROSSIGNAC, J. 2006. Advections with significantly reduced dissipation and diffusion. *IEEE Trans. on Vis. and Comput. Graph. In Press.*.

LAMORLETTE, A., AND FOSTER, N. 2002. Structural modeling of flames for a production environment. *ACM Trans. Graph. (SIGGRAPH Proc.) 21*, 3, 729–735.

LOSASSO, F., IRVING, G., GUENDELMAN, E., AND FEDKIW, R. 2006. Melting and burning solids into liquids and gases. *IEEE Trans. on Vis. and Comput. Graph. 12*, 3, 343–352.

LOSASSO, F., SHINAR, T., SELLE, A., AND FEDKIW, R. 2006. Multiple interacting liquids. *ACM Trans. Graph. (SIGGRAPH Proc.) 25*, 3, 812–819.

MARKSTEIN, G. 1964. *Nonsteady Flame Propagation*. Pergamon Press.

MAZARAK, O., MARTINS, C., AND AMANATIDES, J. 1999. Animating exploding objects. In *Proc. of Graph. Interface 1999*, 211–218.

MELEK, Z., AND KEYSER, J. 2002. Interactive simulation of fire. In *Pacific Graph.*, 431–432.

MELEK, Z., AND KEYSER, J. 2003. Interactive simulation of burning objects. In *Pacific Graph.*, 462–466.

MELEK, Z., AND KEYSER, J. 2005. Multi-representation interaction for physically based modeling. In *ACM Symp. on Solid and Physical Modeling*, 187–196.

MELEK, Z., AND KEYSER, J. 2006. Bending burning matches and crumpling burning paper. In *Poster, SIGGRAPH Proc.*, ACM.

MUSGRAVE, F. K. 1997. Great Balls of Fire. In *SIGGRAPH 97 Animation Sketches, Visual Proceedings*, 259–268.

NEFF, M., AND FIUME, E. 1999. A visual model for blast waves and fracture. In *Proc. of Graph. Interface 1999*, 193–202.

NGUYEN, D., FEDKIW, R., AND KANG, M. 2001. A boundary condition capturing method for incompressible flame discontinuities. *J. Comput. Phys. 172*, 71–98.

NGUYEN, D., FEDKIW, R., AND JENSEN, H. 2002. Physically based modeling and animation of fire. *ACM Trans. Graph. (SIGGRAPH Proc.) 29*, 721–728.

O'BRIEN, J., AND HODGINS, J. 1999. Graphical modeling and animation of brittle fracture. In *Proc. of SIGGRAPH 1999*, 137–146.

OSHER, S., AND SETHIAN, J. 1988. Fronts propagating with curvature-dependent speed: Algorithms based on Hamilton-Jacobi formulations. *J. Comput. Phys. 79*, 12–49.

PEGORARO, V., AND PARKER, S. G. 2006. Physically-based realistic fire rendering. In *Eurographics Workshop on Natural Phenomena (2006)*, E. Galin and N. Chiba, Eds., 237–244.

PERRY, C., AND PICARD, R. 1994. Synthesizing Flames and their Spread. *SIGGRAPH 94 Technical Sketches Notes* (July).

RASMUSSEN, N., NGUYEN, D., GEIGER, W., AND FEDKIW, R. 2003. Smoke simulation for large scale phenomena. *ACM Trans. Graph. (SIGGRAPH Proc.) 22*, 703–707.

RUSHMEIER, H. E., HAMINS, A., AND CHOI, M. 1995. Volume Rendering of Pool Fire Data. *IEEE Comput. Graph. and Appl. 15*, 4, 62–67.

SELLE, A., RASMUSSEN, N., AND FEDKIW, R. 2005. A vortex particle method for smoke, water and explosions. *ACM Trans. Graph. (SIGGRAPH Proc.) 24*, 3, 910–914.

SELLE, A., FEDKIW, R., KIM, B.-M., LIU, Y., AND ROSSIGNAC, J. 2007. An unconditionally stable maccormack method. *J. Sci. Comput. in review. http://graphics.stanford.edu/~fedkiw/*.

STAM, J., AND FIUME, E. 1995. Depicting Fire and Other Gaseous Phenomena Using Diffusion Process. In *Proc. of SIGGRAPH 1995*, 129–136.

STAM, J. 1999. Stable fluids. In *Proc. of SIGGRAPH 99*, 121–128.

YAO, J., AND STEWART, D. S. 1996. On the dynamics of multi-dimensional detonation. *J. Fluid Mech. 309*, 225–275.

YNGVE, G. D., O'BRIEN, J. F., AND HODGINS, J. K. 2000. Animating explosions. In *Proc. of ACM SIGGRAPH 2000*, 29–36.

ZHAO, Y., WEI, X., FAN, Z., KAUFMAN, A., AND QIN, H. 2003. Voxels on fire. In *Proc. of IEEE Vis.*, 271–278.